Lattice dynamic of alpha -quartz. II. Theory

1993 J. Phys.: Condens. Matter 5 6155

(http://iopscience.iop.org/0953-8984/5/34/004)

J. Phys.: Condens. Matter 5 (1993) 6155–6164. Printed in the UK

Lattice dynamics of α-quartz: II. Theory

H Schober†‡§, D Strauch§, K Nützel§ and B Dorner‡

† Kernforschungszentrum Karlsruhe, D-76021 Karlsruhe, Federal Republic of Germany
‡ Institut Laue-Langevin, F-38042 Grenoble Cedex, France
§ Institut für Theoretische Physik, Universität, D-93053 Regensburg, Federal Republic of Germany

Received 22 April 1993, in final form 16 June 1993

Abstract. The recently determined phonon dispersion curves of α-quartz have been analysed with various polarizable-ion, bond-charge and shell models, the shell models giving a very satisfactory account of the dispersion curves as well as of the scattering intensities. Due to the use of interatomic potentials the number of free model parameters can be kept small. Investigating the dielectric constants in the framework of the developed shell models yields an ionic charge of about $-2e$ for the oxygen ion, indicating a strongly ionic crystal. The polarizability of the O^{2-} pseudo-ion in quartz should be close to 1.8 Å^3. The physical significance of the obtained potentials has been tested by studying the equilibrium conditions. It turns out that additional valence forces of the Keating type improve the fulfillment of the equilibrium conditions, but that it is not possible to satisfy them completely.

1. Introduction

The bonding between the atoms of a solid is reflected in its vibrational properties. The reasons why the bonding of silicon and oxygen is of particular interest have already been outlined in the preceding paper [1] (hereafter referred to as I). This interest has led to an extensive experimental investigation of the phonon dispersion relations in α-quartz (SiO_2) (see I).

In the present paper we will analyse the experimental data using various phenomenological lattice dynamical models. Particular effort is made to gain insight into the dynamical response of the oxygen ion. The oxygen ion has been the subject of extensive lattice dynamical investigations for many years, for example in the context of the ferroelectric perovskite-type crystals [2, 3]. These investigations have recently received renewed interest due to the advent of ceramic superconductors [4, 5].

To date several attempts have been made to describe the lattice dynamics of α-quartz. Kleinman and Spitzer [6] have extensively investigated the Γ-point eigenfrequencies and eigenvectors using a valence-force field model. Model calculations of the dispersion curves have been performed by Elcombe [7] and Barron and co-workers [8] using Born–von Kármán and rigid-ion models, and by Striefler and Barsch [9] who have included angular forces of the Keating [10] type. These models have given a very reasonable description of the low-frequency ($\nu < 8$ THz) modes.

To our knowledge there have been two attempts to take into account the oxygen polarizability. Iishi [11] has fitted a polarizable-ion model to the optical data. Sanders and co-workers [12] have adjusted an extended shell model to the elastic and dielectric constants; however, the high-frequency dielectric constants used in [12] do not agree with the ones

0953-8984/93/346155+10$07.50

determined by Gervais and Piriou [13]. In an extended shell model the equilibrium position of the oxygen shell is displaced with respect to its core. As Sanders and co-workers [12] do not indicate to which oxygen ion in the unit cell the communicated displacements refer to, it was impossible for us to investigate their model further. In the course of the present experiments it has turned out that the higher-frequency modes are rather poorly reproduced by either of the above-mentioned models. We have thus investigated various bond-charge [14] and shell models to improve the theoretical description of the experimental dispersion curves.

After a short outline of the crystal structure in section 2 model descriptions of the dispersion curves will be given in section 3. We have paid special attention to the charges and polarizabilities and the resulting dielectric properties of the models. As this involves the introduction of a rather general formalism it will be dealt with only briefly in section 4, the main discussion following in a separate publication [15]. The extent to which our various models fulfill the equilibrium conditions will be discussed in section 5.

A preliminary account of this work has been published elsewhere [16].

2. Crystal structure

The low-temperature modification of quartz (α-quartz) is built up of slightly distorted SiO_4 tetrahedra which are linked by common oxygen ions at the corners. The crystal structure is hexagonal, and there is a structural phase transition from the high-temperature β phase to the low-temperature α phase at $T = 846$ K. In β-quartz the silicon ions form a sixfold screw axis, which is reduced to a threefold screw axis in α-quartz due to a rotation and additional distortion of the SiO_4 tetrahedra. A projection of the atom positions on the basal plane is shown in figure 1. The numbering of atoms is that used in [8], and their coordinates are given in table 1. The structure of α-quartz is defined by the two lattice constants plus four structural parameters. Although our experiments have been performed at a temperature of 20 K we have used throughout this work the structural parameters of Wright and Lehmann [17] as deduced from neutron diffraction data at room temperature. These parameters are in good agreement with the ones deduced from x-ray experiments [18].

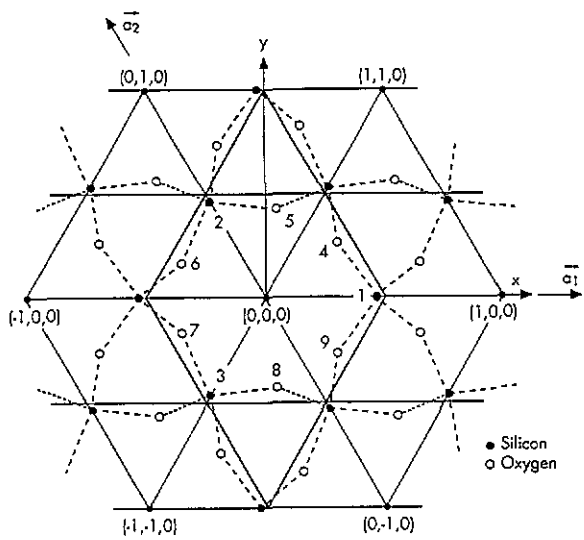

Figure 1. Projection of the atomic positions of levorotatory α-quartz onto the basal plane. The numbering of the atoms is identical to the one used in the text and in table 1; after Barron and co-workers [8]. The numbers in parentheses indicate neighbouring unit cells.

Table 1. Cartesian coordinates of the atomic positions in α-quartz using the structural parameters of [17]. The atoms are numbered as in [8]; a_1, a_2 and a_3 are the hexagonal Bravais vectors.

#	x (Å)	y (Å)	z (Å)
a_1	4.9134	0.0000	0.0000
a_2	−2.4567	4.2551	0.0000
a_3	0.0000	0.0000	5.4052
1 (Si)	2.3098	0.0000	0.0000
2 (Si)	−1.1549	2.0003	3.6035
3 (Si)	−1.1549	−2.0003	1.8017
4 (O)	1.3748	1.1387	0.6438
5 (O)	0.2987	1.7599	2.9597
6 (O)	−1.6735	0.6212	4.2472
7 (O)	−1.6735	−0.6212	1.1580
8 (O)	0.2987	−1.7599	2.4455
9 (O)	1.3748	−1.1387	−0.6438

3. Model calculations

We have investigated various phenomenological lattice-dynamical models. The model parameters have been determined by a least-squares fit to all the measured frequencies. Simple Born–von Kármán-type models, which successfully reproduce the lower phonon branches, cannot give a satisfactory description of the large LO–TO splitting in α-quartz. We have excluded these models from further investigation.

Readjusting the rigid-ion models of Elcombe [7], Barron and co-workers [8] and Striefler and Barsch [9] has given only marginal improvement. In particular, it was not possible to reproduce the marked dispersion of the three uppermost branches in the z direction (see figure 2 of I) nor the scattering intensities. The same is true for the polarizable-ion model of Iishi [11].

By introducing an adiabatically moving shell at the site of the oxygen ion several models with differing short range interactions could be found all giving a very satisfactory description of the experimental phonon data including the scattering intensities. Out of these shell models we will here only discuss the ones showing significant differences. In all versions of the shell model the short-range two-particle interactions have been taken as axially symmetric and their range as limited to the nearest neighbours. In the models SM(1) and SM(2) the force constants for the different oxygen–ion pairs—where the word ion stands for oxygen or silicon respectively—are assumed to be identical despite the differences in bond length (see table 2). Please note that, in contrast to all the other models, no interaction between silicon ions is assumed for model SM(1).

Table 2. Nearest-neighbour distances in α-quartz.

#	Ion pair	r_{ik} (Å)
1	Si(1)–O(4)	1.6079
2	Si(1)–O(6)	1.6100
3	O(4)–O(7)	2.6154
4	O(4)–O(9)	2.6161
5	O(4)–O(5)	2.6282
6	O(4)–O(6)	2.6444
7	Si(1)–Si(2)	3.0572

If we discard models with individual force constants for all the symmetrically inequivalent interactions because of the substantial increase in free parameters, the only way left to account for different nearest-neighbour distances is the use of potentials. In the case of models SM(3) and SM(4), we have employed simple Born–Mayer potentials of the form

$$V(r) = V\mathrm{e}^{-r/a} \tag{1}$$

both for the silicon–oxygen as well as the oxygen–oxygen interactions.

While in models SM(1) and SM(2) only the oxygen ion is assumed to be polarizable, in models SM(3) and SM(4) the polarizability of the silicon ion is taken into account, too. The reason for this was mainly to facilitate numerical calculations. As it turned out the polarizability of silicon could be kept constant at the value of 0.03 Å^3 as given by Delgarno [19]. Model SM(4) contains an additional bond-bending force of the Keating [10] type (see (2) below).

The model parameters of the four models SM(1)–SM(4) as adjusted to the experimental frequencies are listed in table 3 along with the mean deviation $\Delta\nu$ from the experimental frequencies. From the model parameters we have calculated the high-frequency dielectric constants which are given in table 4.

The model dispersion curves of shell model SM(4) can be compared with the experimental data in figures 2 and 3 of I.

The agreement of model results with the experimental scattering intensities is also rather gratifying, as an example see figure 2. The eigenvector exchange is clearly visible.

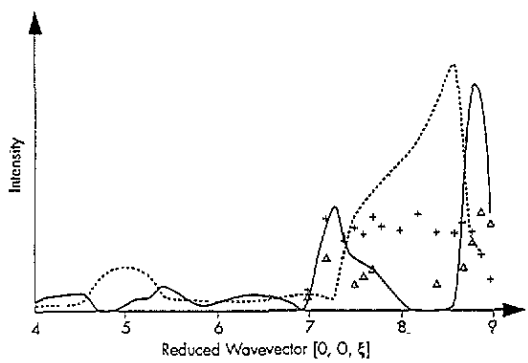

Figure 2. Inelastic neutron scattering intensities for the ninth (theory: full curves; experiment: triangles) and tenth branch (theory: broken curves; experiment: asterisks) of the T_1-representation as a function of reduced wavevector in the Γ–K–M direction. The even numbers indicate consecutive Brillouin-zone centres (Γ-points) and the odd numbers the Brillouin-zone boundaries (M-points). The eigenvector exchange is clearly visible. The theoretical curves were obtained with model SM(1).

As it turns out, the range of the potentials which is determined by the decay constant a in (1) is much the same for quite different models (see table 3). This is particularly true for the silicon–oxygen interaction where the value of a(Si–O) is identical for models SM(3) and SM(4) while the potential strength V(Si–O) differs by 20%. There is a certain degree of indeterminacy of the strength V(O–O) of the oxygen–oxygen potential as long as one does not fix a(O–O). Compared to oxygen–oxygen potentials in e.g. perovskites [20] the parameter a(O–O) is large in all our models. This implies that the derived force constants vary appreciably even for the rather small differences in the bond lengths. As the parameter a also determines the ratio of longitudinal to transverse force constants, its value may in principle depend upon whether or not the central forces have to simulate covalent interactions. Therefore, one should not put too much physical interpretation into the value of a(O–O).

Table 3. Parameters of four shell models SM(1)–SM(4). L and T are the longitudinal and transverse force constants. The superscripts R, S and T indicate whether the interaction is acting between cores, cores and shells, or shells respectively. The interactions are numbered according to table 2. Z is the ionic charge. Y the shell charge, and α the free-oxygen polarizability. V and a are the amplitude and decay constant of the Born–Mayer potentials, see (1); β and β' are the Keating parameters, see (2). Si–O–Si stands for the intertetrahedral angle (143.6°) with oxygen at the apex, O–Si–O for the intratetrahedral angles (108.7° and 110.5°) with silicon at the apex. All Keating interactions are assumed to act between the respective cores only. Parameters marked by an asterisk have been kept fixed. $\Delta\nu$ is the mean square deviation of the calculated frequencies from the experimental frequencies in tables 2–5 of the preceding paper. # is the number of free parameters.

Interaction		Unit	SM(1)	SM(2)	SM(3)	SM(4)
1, 2	L^T	Nm^{-1}	856.2	1150.0		
	T^T	Nm^{-1}	−72.2	−123.0		
	V^S	eV			6631	7800
	a^S	Å			0.209	0.209
3, 4, 5, 6	L^S	Nm^{-1}	47.3	53.5		
	T^S	Nm^{-1}	−9.7	−15.0		
	V^S	eV			500	240
	a^S	Å			0.389	0.430
7	L^R	Nm^{-1}		−77.4		
	T^R	Nm^{-1}		−9.4		
	L^S	Nm^{-1}			−55.0	−127.6
	T^S	Nm^{-1}			0.0	−12.1
	Z(O)	e	−1.42	−1.85	−1.77	−2.00*
	Y(O)	e	−3.34	−3.13	−3.00	−3.13
	Y(Si)	e			−8.0*	−8.0*
	α(O)	$Å^3$	0.80	1.37	1.19	1.86
	α(Si)	$Å^3$			0.03*	0.03*
	β(Si–O–Si)	Nm^{-1}				5.16
	β'(Si–O–Si)					1.00*
	β(O–Si–O)	Nm^{-1}				1.51
	β'(O–Si–O)					2.2
	#		7	9	9	11
	$\Delta\nu$	THz	0.31	0.30	0.33	0.29

Adding a van der Waals interaction of the form $-C/r^6$ between the oxygen shells gives a slightly better fit. As the van der Waals forces are due to induced dipoles we did not limit them to first neighbours only but introduced them between all oxygen pairs. Actually, for a distance larger than 5 Å the force constants become so small that they can be neglected. We have found values for the constant C between 30–100 eV Å^6. These values are of the same order as those found by Sanders and co-workers [12] for quartz and by Mackrodt and Steward [21] for sapphire. The large uncertainties in C stem from the strong correlation between the van der Waals and Born–Mayer parameters such that it is impossible to determine the strength of the two potentials independently. This is not at all surprising given the small differences in the oxygen–oxygen bond lengths (see table 2).

Due to the adiabatic motion of the shells, indirect interactions between second and further neighbours are induced even if there are no direct interactions between these ions. In order to assess the range of these indirect interactions mediated by the shells we have calculated the trace of the dynamical matrix for the z and x directions (see [22]). Within numerical accuracy the trace is found to be independent of the wavevector. This implies that there are no induced interactions with a range larger than the dimensions of the primitive cell except for electrostatic interactions which do not enter the trace due to the Poisson

Table 4. Dielectric constants as derived from the parameters of four shell models SM(1)–SM(4) compared to the experimental values ([13,29]: infrared reflectivity; [32]: method of substitution). ϵ^{∞}_{xx}, ϵ^{0}_{xx} and ϵ^{∞}_{zz}, ϵ^{0}_{zz} are the two independent elements of the high-frequency and static dielectric constant, respectively.

	SM(1)	SM(2)	SM(3)	SM(4)	Expt
ϵ^{∞}_{xx}	1.57	1.95	1.83	2.36	2.356 [13,29]
ϵ^{∞}_{zz}	1.57	1.95	1.84	2.37	2.383 [13,29]
ϵ^{0}_{xx}	2.89	3.47	3.51	4.03	4.4 [13], 4.32 [29], 4.52 [32]
ϵ^{0}_{zz}	2.89	3.51	3.68	4.00	4.5 [13], 4.56 [29], 4.64 [32]

equation [23].

Even though the four shell models describe the dispersion curves comparably well, there is generally some difficulty to reproduce the slope of all the acoustic branches simultaneously. This difficulty increases with increasing ionic charge. We believe that this is connected to an insufficient description of the covalent bonding in quartz. An appreciable improvement is achieved by adding angle-bending forces derived from potentials of the Keating type [10]:

$$V_{\text{Keating}} = -\sum_{ii'i''} \beta_{i'ii''} \frac{(\boldsymbol{r}_{ii'} \cdot \boldsymbol{r}_{ii''} - \beta'_{i'ii''} \boldsymbol{r}^{0}_{ii'} \cdot \boldsymbol{r}^{0}_{ii''})^2}{\boldsymbol{r}^{0}_{ii'} \cdot \boldsymbol{r}^{0}_{ii''}}. \tag{2}$$

Here, $\boldsymbol{r}_{ii'}$ is the vector pointing from particle i to particle i', and the superscript 0 denotes its equilibrium positions. As pointed out by Sanders and co-workers [12] the addition of valence forces improves the description of the acoustic branches but neither are the necessary central potentials drastically different nor the optical branches substantially improved. It should be noted that the slopes of the measured dispersion curves for the acoustic modes in the x direction do not coincide with the sound velocities derived from the elastic constants [24]. This causes a major problem as models fitted to the elastic constants cannot correctly reproduce the acoustic branches measured by inelastic neutron scattering and vice versa. Dorner and co-workers [25] explain this discrepancy by the different slopes in the zero- and first-sound regime.

We have also investigated bond-charge models [14] with the bond charges situated along the lines connecting neighbouring Si and O ions. The quality of the fits are worse than for the shell models. The bond-charge positions in quartz are not constrained by symmetry, and their choice poses a major problem. In fact, electronic density calculations [26] indicate that the maxima of the p-like bands, which might be associated with bond charges, are found slightly off the line connecting a silicon with an oxygen atom. We have discarded these off-bond positions as they introduce two more parameters. Rustagi and Weber [27] have, however, pointed out that the success of their bond-charge model for the III–V semiconductors depends critically on the bond-charge position (along the bond). The different importance of bond charges for the lattice dynamics of the elemental and III–V semiconductors [27] on the one hand and for that of quartz on the other may be due to the different electronic density distributions [26,28]. In quartz the total electronic density is centred on the oxygen ions, and there are no strong maxima along the bonds as is the case for the semiconductors. In addition, the main electronic transitions in quartz are localized at the oxygen ion while in the semiconductors these transitions are taking place between bands having most of the charge density not at the ion but at the bonding sites.

The introduction of interactions between second-nearest oxygen pairs as used by Barron and co-workers [8] has not resulted in any sizable improvement of the overall phonon

dispersion and may not make sense if the difference in the first-neighbour distances is not accounted for.

4. Charges and polarizability

The most striking feature of the models is the wide range of values for the ionic charge and for the oxygen polarizability ($-2.0e < Z(O) < -1.4e$; $0.8\,\text{Å}^3 < \alpha(O) < 1.9\,\text{Å}^3$). The two parameters are, however, strongly correlated, and we have found a nearly linear dependence of the polarizability on the ionic charge for charges smaller than $-1.9e$ (see [15], figure 1). This scaling of the polarizability with charge can be understood as resulting from the strong LO–TO splitting. Comparing the LO–TO splitting as reproduced by different models is not trivial in the case of complex structures like quartz as a large number of polar modes contribute to it. In [15] we introduce a measure, i.e. a scalar quantity characterizing the LO–TO splitting, which can be calculated without diagonalization of the dynamical matrix thus making an approximate analytical treatment of the LO–TO splitting possible. Qualitatively, given an ionic charge Z we can analytically determine the value of the polarizability α necessary to screen Z in such a way that we obtain the desired LO–TO splitting.

All our models reproduce the LO–TO splitting equally well. In order to investigate the contribution due to the electronic screening we have determined the high-frequency dielectric constant for all our shell models. Due to its hexagonal symmetry the dielectric tensor of quartz is diagonal with only two independent components. Experimentally [13], the high-frequency dielectric constant of quartz is nearly isotropic. This is also reproduced by all our models. In [15] we come back to this point and its implications. The values for the high-frequency dielectric constants as obtained from the shell models SM(1)–SM(4) range from 1.34–2.37, which is to be compared with the experimental value of about 2.37 [13, 29], see table 4. The dielectric constant predicted by the model SM(4) turns out to coincide with the experimental value. SM(4) with the ionic charge of the oxygen fixed at $-2e$ can therefore be considered to give a reasonable model description of the electronic polarizability.

As we show in [15] the dielectric constant scales nearly linearly with the polarizability of the oxygen ion. In order for the high-frequency dielectric constant to attain the experimental value the polarizability α of the (hypothetical) free oxygen ion has to assume values between 1.7–2.0 Å^3.

Note that this result is independent of any special model and only relies on the validity of shell models for the description of the lattice dynamics of α-quartz in general. The uncertainty in α stems from the fact that the polarizability is modified (generally reduced) by the short-range forces which act on the shells and thus influence the (hypothetical) value for the polarizability of the free oxygen ion. Knowing the value of the polarizability we can use the scaling of the charge with polarizability to place limits on the ionic charge of the oxygen ion in quartz. It must be very close to $-2e$.

The polarizable-ion model of Iishi [11] with a free-oxygen polarizability of 1.38 Å^3 also reproduces the dielectric constant correctly. However, it does not account for the LO–TO splitting.

5. Equilibrium conditions

The investigation of the equilibrium conditions requires a knowledge of the first derivatives of the interionic potentials. For the shell models SM(3) and SM(4) there are explicit (Born–Mayer and Keating) potentials. For the other models the short-range central potentials can

be deduced from the assumption that the model force constants are related to the first and second derivatives of such potentials. In both cases it can be shown immediately that in all our models residual forces must act on the ions whatever values one chooses for the short-range model parameters. It is impossible to satisfy simultaneously all six equilibrium conditions corresponding to the six structural parameters of α-quartz with the limited number of parameters which we have used to describe the dynamics. Only in the case in which one assumes zero charge in these models and in addition neglects the distortion of the tetrahedra can the equilibrium conditions be fulfilled. This reflects the fact that with increasing charge it becomes more and more difficult to balance the static Coulomb forces by short-range forces; this is related to the difficulty in the model description of the acoustic branches. Additional valence forces of the Keating type with $\beta' = 1$ in (2) do not enter the equilibrium conditions. This is due to the fact that the Keating potential is rotationally invariant and, therefore, does not contribute to the equilibrium conditions. However, the incorporation of a Keating potential results in a change of the other short-range model parameters when they are adjusted to the dispersion curves. Thus, there is an indirect influence of the Keating potential. This is actually the case for the model SM(4) in which Keating interactions are included and in which the equilibrium conditions are much less violated than in the other models. This does not alter the fact that an exact fulfillment of the equilibrium conditions is still impossible.

Therefore, we conclude that the force constants of our models should be considered as effective force constants arising from a multitude of interionic potentials which do not necessarily have to be central and which are difficult to determine from lattice dynamics alone. This is not surprising if one considers the fact that the chemical bond in α-quartz is of partially covalent character.

For the investigation of the equilibrium conditions in α-quartz we have assumed that there is no static dipole moment at the oxygen site. This is inconsistent with the fact that due to the low symmetry of the structure the electric field at the oxygen sites is non-vanishing. In conjunction with the rather high oxygen polarizability this must inevitably lead to static dipole moments which have to be included in the equilibrium conditions. In shell models such dipole moments can be generated if the shell equilibrium positions are allowed to differ from those of their respective cores [12]. In quartz this would involve three additional structural parameters and three additional equilibrium conditions. Even if the equilibrium conditions of the shells can be calculated from an assumed potential derived from the fitted force constants it seems that the other equilibrium conditions still cannot be fulfilled. Since the true interionic potentials are unknown we have not followed this route. (In the case of β-quartz the direction of the static dipole moment is fixed, and the oxygen position is determined by only one parameter.)

We have found a rather strong influence of the structural parameters on the lattice dynamics: retaining, for example, the parameters of model SM(2) but replacing the structural parameters of Wright and Lehmann [17] by those used in [8] leads to differences in the calculated frequencies of up to 0.4 THz for certain branches. Please note that model SM(2) is a force constant model. The changes in the structural parameters do therefore not influence the strength of the interactions. Even stronger changes in the dispersion relations occur when applying the potentials and force constants found for α-quartz to the β-quartz structure. Without corrections this procedure results for nearly all our models in an unstable situation and even after significant modifications have been made to the models the phonon data available for β-quartz [13, 30, 31] are described only poorly. In this context it is interesting to note that small changes (0.02 Å) of the shell position can change a model from stable

to unstable. Therefore, we conclude that the static dipole moment on the oxygen ion may play an important role in the mechanism of the phase transition.

6. Conclusion

The investigation of the phonon spectrum has shown that α-quartz is a highly ionic crystal. The covalent part of the bonding shows up mainly in the violation of the equilibrium conditions for models with only central interactions. This also leads to difficulties with the description of the acoustic branches. Otherwise, the overall dispersion relations of simple shell models with central forces between nearest neighbours show very good agreement with experiment for the two measured directions. Due to the violation of the equilibrium conditions these force constants and potentials must be regarded as effective in the sense that they contain an appreciable amount of valence interactions not explicitly included in our models.

Of all the models SM(4) is outstanding, since in addition to a very good reproduction of the optic branches it gives the best description of the acoustic branches as well as the correct value for the high-frequency dielectric constant. In model SM(4) the oxygen charge is not a free parameter but fixed at $-2e$. Like all the other models (with an ionic charge close to $-2e$) in model SM(4) one finds strong short-range force constants between the nearest silicon–silicon neighbours in order to balance the Coulomb forces. As this interaction is much stronger than one would expect from the large bond length (see table 2) it seems that it simulates valence forces associated with the Si–O–Si angle, hinting at the importance of these forces for the lattice dynamics of α-quartz.

The success of model SM(4) combined with the general investigation of the LO–TO splitting and the dielectric constants indicates that the oxygen ion in α-quartz is very close to an O^{2-} configuration with a free-oxygen polarizability between 1.7–1.9 $Å^3$. Very similar values have been found for the oxygen ion in perovskites [2, 3, 20].

Improvements of our models should incorporate a realistic description of the covalent forces in α-quartz. Keating potentials have been found to be only partially successful with this respect. In particular, they are not suited to replace the strong silicon–silicon central interactions mentioned above.

We wish to point out that the above results have only been made possible because the measurements of the phonon branches have been extended up to the highest frequencies. In particular, we have found that the data for one symmetry direction alone are insufficient to establish reliable lattice dynamical models.

Acknowledgments

We are grateful to Dr G Eckold for sending a version of the UNISOFT computer program package [33] prior to publication.

References

[1] Strauch D and Dorner B 1993 *J. Phys.: Condens. Matter* **5** 6149
[2] Axe J D, Shirane G and Müller K A 1969 *Phys. Rev.* B **183** 820
[3] Jannot B, Escribe-Filippini C and Bouillot J 1984 *J. Phys. C: Solid State Phys.* **17** 1329
[4] Kress W, Schröder U, Prade J, Kulkarni A D and deWette F 1988 *Phys. Rev.* B **38** 2906

[5] Pintschovius L, Pyka N, Reichardt W, Rumiantsev A Yu, Mitrofanov N L, Ivanov A S, Collin G and Bourges P 1991 *Physica* C **185–189** 156
[6] Kleinmann D A and Spitzer W G 1962 *Phys. Rev.* **125** 16
[7] Elcombe M M 1967 *Proc. Phys. Soc.* **91** 947
[8] Barron T H K, Huang C C and Pasternak A 1976 *J. Phys. C: Solid State Phys.* **9** 3925
[9] Striefler M E and Barsch G R 1975 *Phys. Rev.* B **12** 4553
[10] Keating P N 1966 *Phys. Rev.* **145** 637
[11] Iishi K 1978 *Am. Mineral.* **63** 1190
[12] Sanders M J, Leslie M and Catlow C R A 1984 *Chem. Commun.* 1271
[13] Gervais F and Piriou B 1975 *Phys. Rev.* B **11** 3944
[14] Weber W 1977 *Phys. Rev.* B **15** 4789
[15] Schober H and Strauch D 1993 *J. Phys.: Condens. Matter* **5** 6165
[16] Dorner B, Strauch D, Schober H and Nützel K 1990 *Phonons 89* ed. S Hunklinger, W Ludwig and G Weiss (Singapore: World Scientific) p 76
[17] Wright A F and Lehmann M S 1981 *J. Solid State Chem.* **36** 371
[18] Le Page Y and Donnay G 1976 *Acta Crystallogr.* B **32** 2456
[19] Delgarno A 1962 *Adv. Phys.* **11** 281
[20] Prade J 1989 *Dissertation* Universität Regensburg
[21] Mackrodt W C and Stewart R F 1979 *J. Phys. C: Solid State Phys.* **12** 431
[22] Cowley E R and Okazaki A 1967 *Proc. R. Soc.* A **300** 45
[23] Rosenstock H B 1962 *Phys. Rev.* **129** 1959
[24] McSkimin H J, Andreatch P and Thurston R N 1965 *J. Appl. Phys.* **36** 1624
[25] Dorner B, Grimm H and Rzany H 1980 *J. Phys. C: Solid State Phys.* **13** 6607
[26] Chelikowsky J R and Schlüter M 1977 *Phys. Rev.* B **15** 4020
Bingelli N, Troullier N, Martins J L and Chelikowsky J R 1991 *Phys. Rev.* B **44** 4771
[27] Rustagi K and Weber W 1976 *Solid State Commun.* **18** 673
[28] Walter J P and Cohen M L 1971 *Phys. Rev.* B **4** 1877
[29] Spitzer W G and Kleinman D A 1961 *Phys. Rev.* **121** 1324
[30] Bethke J, Dolino G, Eckold G, Berge B, Vallade M, Zeyen C M E, Hahn T, Arnold H and Moussa F 1987 *Europhys. Lett.* **3** 207
[31] Bates J B and Quist A S 1972 *J. Chem. Phys.* **56** 1528
[32] Fontanella J, Andeen C and Schuele D 1974 *J. Appl. Phys.* **45** 2852
[33] Eckold G, Stein-Arsic M and Weber H J 1987 *J. Appl. Cryst.* **20** 134